

Virulence traits of a serogroup C Meningococcus and isogenic cssA mutant, defective in surface-exposed sialic acid, in a murine model of meningitis

This is the peer reviewed version of the following article:

Original:

Colicchio, R., Pagliuca, C., Ricci, S., Scaglione, E., Grandgirard, D., Masouris, I., et al. (2019). Virulence traits of a serogroup C Meningococcus and isogenic cssA mutant, defective in surface-exposed sialic acid, in a murine model of meningitis. INFECTION AND IMMUNITY, 87(4), e00688-18-e00688-18 [10.1128/IAI.00688-18].

Availability:

This version is available <http://hdl.handle.net/11365/1108407> since 2020-05-13T15:32:46Z

Published:

DOI: <http://doi.org/10.1128/IAI.00688-18>

Terms of use:

Open Access

The terms and conditions for the reuse of this version of the manuscript are specified in the publishing policy. Works made available under a Creative Commons license can be used according to the terms and conditions of said license.

For all terms of use and more information see the publisher's website.

(Article begins on next page)

1 **Virulence traits of serogroup C meningococcus and isogenic *cssA* mutant, defective in**
2 **surface-exposed sialic acid, in a murine model of meningitis**

3
4 **Roberta Colicchio^a, Chiara Pagliuca^a, Susanna Ricci^b, Elena Scaglione^a, Denis Grandgirard^c,**
5 **Ilias Masouris^d, Fabrizio Farina^e, Caterina Pagliarulo^f, Giuseppe Mantova^a, Laura**
6 **Paragliola^g, Stephen L. Leib^c, Uwe Koedel^d, Gianni Pozzi^b, Pietro Alifano^h, Paola**
7 **Salvatore^{a,g,i,*}.**

8
9 ^aDepartment of Molecular Medicine and Medical Biotechnology, Federico II University, Naples,
10 Italy; ^bLaboratory of Molecular Microbiology and Biotechnology (LAMMB), Department of
11 Medical Biotechnologies, University of Siena, Siena, Italy; ^cInstitute for Infectious Diseases,
12 University of Bern, Bern, Switzerland; ^dDepartment of Neurology, Ludwig-Maximilians University
13 of Munich, München, Germany; ^eDepartment of Law, Economics, Management and Quantitative
14 Methods (DEMM), University of Sannio, Benevento, Italy; ^fDepartment of Science and
15 Technology, Sannio University, Benevento, Italy; ^gDepartment of Integrated Activity of Laboratory
16 Medicine and Transfusion, Complex Operative Unit of Clinical Microbiology, University Hospital
17 Federico II, Naples, Italy; ^hDepartment of Biological and Environmental Sciences and
18 Technologies, University of Salento, Lecce, Italy; ⁱCEINGE, Biotechnologie Avanzate s.c.ar.l.,
19 Naples, Italy.

20
21 **Keywords:** *Neisseria meningitidis*; meningoenkephalitis; sialic acid; capsule; LOS; meningitis
22 mouse models; *corpus callosum*.

23
24 **Address correspondence to Paola Salvatore:** psalvato@unina.it

25
26 **Running Title:** Virulence of meningococcal isogenic *cssA* mutant

27 **ABSTRACT**

28 In serogroup C *Neisseria meningitidis*, the *cssA* (*siaA*) gene codes for an UDP-*N*-acetylglucosamine
29 2-epimerase that catalyzes the conversion of UDP-*N*-acetyl- α -D-glucosamine into *N*-acetyl-D-
30 mannosamine and UDP in the first step in sialic acid biosynthesis. This enzyme is required for the
31 biosynthesis of the (α 2 \rightarrow 9)-linked polysialic acid capsule and for lipooligosaccharide (LOS)
32 sialylation. In this study, we have used a reference serogroup C meningococcal strain and an
33 isogenic *cssA* knockout mutant to investigate the pathogenetic role of surface-exposed sialic acids
34 in a model of meningitis based on intracisternal inoculation of BALB/c mice. Results confirmed the
35 key role of surface-exposed sialic acids in meningococcal pathogenesis. The 50% lethal dose (LD₅₀)
36 of the wild type strain 93/4286 was about four orders of magnitude lower than that of the *cssA*
37 mutant. Compared to the wild type strain, the ability of this mutant to replicate in brain and spread
38 systemically was severely impaired. Evaluation of brain damage evidenced a significant reduction
39 in cerebral hemorrhages in mice infected with the mutant in comparison with those challenged with
40 the wild type strain. Histological analysis showed the typical features of bacterial meningitis,
41 including inflammatory cells in the subarachnoid, perivascular and ventricular spaces especially in
42 animals infected with the wild type. Noticeably, 80% of mice infected with the wild type strain
43 presented with massive bacterial localization and accompanying inflammatory infiltrate in the
44 *corpus callosum*, indicating high tropism of meningococci exposing sialic acids toward this brain
45 structure and a specific involvement of the *corpus callosum* in the mouse model of meningococcal
46 meningitis.

47

48 INTRODUCTION

49 *Neisseria meningitidis* is a leading cause of sepsis and meningitis worldwide in humans. Invasive
50 disease is preceded by asymptomatic nasopharyngeal colonization occurring in up to 18% of the
51 normal population. In some individuals this common transitory colonizer is able to breach the
52 mucosal barrier, get into bloodstream and multiply uncontrollably, and finally cross the blood-brain
53 barrier (BBB) to cause meningitis. Both host and bacterial factors seem to be involved in this switch
54 from harmless transitory colonization to devastating disease (1).

55 *N. meningitidis* infects only humans because of the high specificity of both meningococcal
56 surface structures and iron uptake systems for human receptors and transport proteins (2-4). The
57 lack of valuable animal models of disease due to the narrow host range, along with the
58 meningococcal high degree of genetic (phase and antigenic) variation of surface structures, have
59 greatly hindered progress in understanding the pathogenesis of meningococcal disease and
60 developing effective vaccines. Much of our knowledge about cellular and molecular biology of this
61 human pathogen and its virulence determinants including capsular polysaccharide,
62 lipooligosaccharide, and a number of surface-adhesive and secreted proteins comes from cell and
63 organ culture systems or animal models that, however, fail to reproduce the complexity of the
64 infectious cycle in the human host (5).

65 Among the virulence factors described so far, surface-exposed sialic acids occupy a prominent
66 position (6,7). Thirteen *N. meningitidis* serogroups have been described on the basis of serologic
67 differences of the capsular polysaccharides; of these, five (A, B, C, Y and W-135) cause the
68 majority of invasive disease. According to recent WHO data, meningococcal serogroup C is still
69 one of the most widespread serogroups in the world (Invasive Meningococcal Disease - Serogroup
70 distribution, WHO 2018, <https://www.who.int/emergencies/diseases/meningitis/en/>). Recently, a
71 new meningococcal meningitis clone of serogroup C is expanding in Sub-Saharan Africa,
72 associated with a huge risk of a major epidemic in the next two years (WHO 2018,
73 <https://www.who.int/emergencies/diseases/meningitis/en/>). In addition, since January 2015, in

74 Tuscany, Italy, there was an unexpected increase of invasive meningococcal disease, (a total of 43
75 cases, of whom 10 were fatal), due to infection with serogroup C *N. meningitidis*. Thirty-five out of
76 the samples analysed in this study were confirmed as C:P1.5-1,10-8:F3-6:ST-11 [clonal complex
77 (cc) 11] (8).

78 Among the serogroups responsible for epidemics four of them (B, C, Y and W-135) carry sialic
79 acids in their capsular polysaccharide (5). Sialic acid is also found as a modification (in place of the
80 terminal galactose residue) of the meningococcal LOS in serogroups with a sialic acid-containing
81 capsule (9). The large abundance of surface-exposed sialic acids is associated with virulence and
82 serum resistance to both phagocytosis and complement-mediated killing via alternative pathway
83 activation (10-16) resulting in enhanced survival in the bloodstream and central nervous system
84 (CNS) (17). There is also evidence that the meningococcal polysialic acid capsule is important for
85 bacterial survival within human cells (18), mediates the interaction of bacteria with host cell
86 microtubules during cell infection (19), and protects the bacteria against cationic antimicrobial
87 peptides (CAMP) including human cathelicidin LL-37 (18, 20). On the other hand, expression of
88 the polysialic acid capsule hinders colonization and invasion of the nasopharyngeal barrier by
89 masking adhesins/invasins (21-23). For these reasons, capsular polysaccharide expression is
90 subjected to frequent phase variation via slipped-strand mispairing affecting *cssD* (*siaD*) or *cssA*
91 (*siaA*) (21, 24) or reversible insertion of *IS1301* mobile elements in *cssA* (22) and is tightly
92 regulated at the transcriptional level (25). Loss or down-regulation of polysialic acid capsule
93 expression facilitates meningococcal attachment (18, 22, 23, 26) and biofilm formation, and
94 correlates with the nasopharyngeal carriage in humans (6).

95 In the past, our research group has developed a model of meningococcal meningitis (MM) based
96 on intracisternal (i.cist.) infection of adult mice with mouse-passaged bacteria (27). Survival and
97 clinical parameters of infected mice, and microbiological and histological analyses of the brain
98 demonstrated the establishment of meningitis with features comparable to those of the disease in
99 humans. Meningococci were also found in the blood, spleen, and liver of infected mice, and

100 bacterial loads in different organs were dependent on the infectious dose. The model was used to
101 assess the virulence of a mutant strain deficient in the L-glutamate transporter GltT (27). The aim of
102 the present study was to evaluate the role of surface-exposed sialic acids in the establishment of
103 meningitis and meningoencephalitis in mice when the bacteria are directly injected i.cist using the
104 MM model in mouse. To this purpose, we have used the reference serogroup C meningococcal
105 strain 93/4286 and an isogenic *cssA* knockout mutant defective in UDP-*N*-acetylglucosamine 2-
106 epimerase that catalyzes the first step of sialic acid (*N*-acetylneuraminic acid) biosynthesis, *i.e.*, the
107 conversion of UDP-*N*-acetyl- α -D-glucosamine into *N*-acetyl-D-mannosamine and UDP (28). The
108 50% lethal dose (LD₅₀) of these strains were determined as well as their abilities to replicate in the
109 brain and other organs. To investigate the infectious dynamics and histopathological correlates of
110 the disease in the MM mouse model, histological evaluation, cerebral bleeding analysis and
111 localization of bacteria in brain structures were carried out.

112

113 RESULTS

114 **Construction of a serogroup C *cssA*-defective isogenic mutant.** The isogenic mutant
115 93/4286 Ω *cssA* of the serogroup C reference strain 93/4286 was obtained by insertional inactivation
116 of the *cssA* gene (NMC0054 or NMC_RS00310), coding for the UDP-*N*-acetylglucosamine 2-
117 epimerase (EC 3.2.1.183). In the genome of serogroup C strains, *cssA* is the first gene of the Region
118 A capsule synthesis locus, which comprises the conserved *cssABC* (formally denominated *siaABC*)
119 genes for CMP-*N*-acetylneuraminic acid biosynthesis followed by serogroup C-specific loci, *csc*
120 (*siaD_C*) coding for α 2 \rightarrow 9 polysialyltransferase, and *cssE* (*oat_C*) encoding the *O*-acetyltransferase
121 (29) (Fig. 1A). Southern blot analysis confirmed disruption of the *cssA* gene. By using an *cssA*-
122 specific probe, two *NdeI* DNA fragments of the expected sizes (3,180 bp and 2,183 bp) were
123 detected in the 93/4286 Ω *cssA* strain, compared to a single 791 bp *NdeI* fragment observed in the
124 wild type strain 93/4286 (Fig. 1 B). The absence of capsular polysaccharide expression in the
125 mutant was confirmed by latex slide agglutination test using antibodies against serogroup C
126 meningococci capsular polysaccharide (Supplemental Fig. S1).

128 **Characterization of 93/4286 Ω *cssA* mutant under *in vitro* conditions.**

129 In order to exclude any differences during bacterial replication, the growth rate of wild-type strain
130 93/4286 and its derivative *cssA* mutant was preliminarily analyzed in GC broth at 37°C. The *cssA*
131 mutant exhibited growth curves comparable to those of the wild-type strain with a growth rate (μ =
132 0.97 \pm 0.08) comparable to that of the reference strain (μ = 0.85 \pm 0.06) without any statistically
133 significant difference (Supplemental Fig. S2 and Supplemental Table S1). In GC medium, the *in*
134 *vitro* competition index of *cssA* defective strain was also determined. The growth rate of mutant
135 during the logarithmic phase of growth compared to that of the wild-type strain provided a relative
136 fitness of the mutant of 108% compared to the wild type strain (Table 1). Moreover, the *cssA*
137 mutant had a growth curves and colony morphology similar to those of the wild-type strain even in
138 DMEM medium (Supplemental Fig. S3 and data not shown). In cell culture medium, the growth

139 rate of *cssA* defective mutant ($\mu = 0.25 \pm 0.004$) was comparable to that of wild type strain
140 ($\mu = 0.30 \pm 0.04$) (Supplemental Table S2).

141 In addition, the *cssA* mutant, grown in GC broth, exhibited a slight up-regulation in the
142 expression of virulence-associated surface adhesins, such as pilin (*pilE*, 1.64 ± 0.63 fold change) and
143 non-fimbrial adhesins such as opacity protein (*opa*, 1.66 ± 0.65 fold change), neisserial heparin-
144 binding antigen (*nhbA*, 2.08 ± 0.38 fold change), neisserial adhesin A (*nadA* 2.07 ± 0.36 fold change),
145 adhesin/invasin (*hrpA*, 1.98 ± 0.38 fold change), and factor H binding protein (*fHbp*, 2.08 ± 0.23 fold
146 change) (Supplemental Fig. S4). The difference in the expression of all analyzed genes was not,
147 however, statistically significant.

148
149 **Survival of mice infected with the 93/4286 Δ *cssA* mutant is significantly increased.** The
150 virulence of the *cssA*-defective strain was assessed in the MM model by analyzing animal survival
151 at different bacterial doses. In order to determine the dose lethal for 50% of animals (LD_{50}), three
152 groups of mice were infected by i.cist. injection of 10^4 , 10^5 , and 10^6 cfu of the wild type strain
153 93/4286 or 10^7 , 10^8 , and 10^9 cfu of the mutant strain 93/4286 Δ *cssA*. Preliminary data showed
154 higher survival rates in animals infected with the *cssA*-defective mutant with the same doses used
155 for the wild type strain (data not shown). In accordance with previous results (25), mouse death,
156 weight loss and temperature drop generally occurred within the first 72 h after meningococcal
157 inoculation. Results with the wild type strain 93/4286 indicated that 50% and 16.6% of rodents
158 survived meningococcal challenge with 10^4 and 10^5 cfu, respectively, while all mice died at the dose
159 of 10^6 cfu (Fig. 2A). A significant difference was observed between the three groups (log rank test,
160 $P < 0.05$). In contrast, at the lowest dose of 10^7 cfu, there was 83.3% survival in the group infected
161 with the mutant strain 93/4286 Δ *cssA*, while 50% survival was recorded in mice inoculated with 10^8
162 cfu (Fig. 2B), indicating a 10,000 folds increased LD_{50} of the *cssA*-defective mutant.

163

164 **The 93/4286 Ω *cssA* mutant is severely impaired at replicating in the mouse brain.** To determine
165 the number of meningococci in the brain at different stages of disease, animals were injected i.cist.
166 with 5×10^5 cfu of 93/4286 or 93/4286 Ω *cssA* strains and sacrificed at different time points after
167 challenge (Fig. 3A). A rapid increase in cfu counts was observed for wild type bacteria that reached
168 the highest numbers 24 h after inoculation ($8.519 \log \text{cfu} \pm 0.072$). In contrast, bacterial loads in the
169 brain of mice challenged with the *cssA*-defective mutant progressively dropped over time reaching
170 $2.026 \log \text{cfu} \pm 1.774$ 72 h post infection (Fig. 3A). Bacterial clearance from the infection site
171 occurred in 33.3% of subjects challenged with the mutant, whereas infection was never eradicated
172 from the brain of mice that had received the wild type strain.

173

174 **The *cssA*-defective mutant is cleared systemically from mice with MM.** To evaluate clearance of
175 bacteria from infected mice, two groups of animals were inoculated with 5×10^5 cfu of either
176 93/4286 or 93/4286 Ω *cssA* strains, and bacterial viable counts in the spleen and liver were
177 determined (Fig. 3B). Systemic meningococcal infection caused by the *cssA*-defective mutant was
178 entirely cleared within 48 h from i.cist. challenge, whereas none of the animals inoculated with the
179 wild type had eliminated bacteria from spleen and liver. Two days after inoculation, mean cfu
180 counts of the wild type strain in the spleen and liver were still $3.212 \log \text{cfu} \pm 3.354$ and $6.949 \log$
181 $\text{cfu} \pm 1.37$, respectively. Differences in bacterial loads in the liver between the two animal groups
182 were statistically significant (with a $P < 0.001$).

183

184 **Serogroup C wild type meningococci induced severe MM in mice with preferential**
185 **localization in the *corpus callosum*.** To compare the disease induced by the wild type 93/4286 and
186 *cssA*-defective mutant, histological analysis and bacterial immunostaining were performed on brain
187 slices from infected mice 48 hours after infection.

188 MM was considerably more severe in animals infected with the wild type (Fig. 4A) compared to
189 those challenged with the *cssA*-defective strain (Fig. 4B). Histological analysis showed the typical

190 features of bacterial meningitis, including the presence of inflammatory cells in the subarachnoid
191 (Fig. 4C, black arrowheads), perivascular and ventricular spaces (Fig. 4D, white arrowheads).
192 Vasculitis (Fig. 4C, white arrowheads) and hemorrhages (Fig. 4A, black arrows) were observed
193 mainly in animals infected with the wild type strain. Interestingly, inflammatory infiltrates were
194 detected in the *corpus callosum* (Fig. 4E). Indeed, 80% of mice infected with the wild type
195 presented with severe inflammation in the *corpus callosum* (Fig. 4E, white arrowheads). In contrast,
196 except for one mouse, no massive evident inflammatory infiltrates, but only few immune cells,
197 could be observed in the *corpus callosum* of animals infected with the mutant strain (Fig. 4F, white
198 arrowheads). The presence and localization of bacteria was further investigated by
199 immunofluorescence. In animals infected with the wild type 93/4286 strain, immunoreactivity with
200 a meningococcal antiserum showed was mostly detected in the *corpus callosum* (Fig. 5A-B), in
201 association with neutrophils in the ventricles (Fig. 5C) or on the meninges (data not shown). A
202 positive signal associated with the cells lining the ventricle or possibly cells from the choroid plexus
203 was also detected (data not shown). In contrast, immunostaining of meningococci revealed no
204 signal in the *corpus callosum* of animals infected with the *cssA*-defective mutant (Fig. 5 D-E). A
205 weak immunoreaction was detected in association with cells in the ventricles (Fig. 5F) or on the
206 meninges (data not shown).

207
208 **Mice infected with the *cssA*-defective mutant showed reduced intracerebral hemorrhages.** In
209 a previous study, cerebral bleeding was identified as a consistent readout in the brain of mice with
210 MM (30). To perform a quantitative analysis of brain bleeding, the number and area of cerebral
211 bleedings were determined in mice infected by the wild type or the *cssA*-defective strains. In
212 accordance with histological data, results showed a significant reduction both in macroscopical
213 assessment of cerebral haemorrhages (Fig. 6A), in the number of bleeding spots (Fig. 6B; $P=0.01$)
214 and in the haemorrhagic area (Fig. 6C; $P=0.048$) in mice challenged with *cssA*-defective bacteria.

215

216 DISCUSSION

217 Sialic acids are a family of nine-carbon carboxylated sugars, which include more than 50
218 different members classified based on various substituents on carbon 4, 5, 7, 8, and 9. The
219 substituent on carbon 5 defines the four most common types of sialic acids: neuraminic acid (Neu),
220 N-acetylneuraminic acid (Neu5Ac), N-glycolylneuraminic acid (Neu5Gc), and 2-keto-3-deoxy-
221 nonulosonic acid (Kdn). They can be found as terminal sugars of glycoconjugates such as
222 glycoproteins and glycolipids on cell surface of vertebrates and higher invertebrates (31, 32). By
223 modulating contact-dependent mechanisms, sialic acids and their metabolism play key roles in
224 many physiological and pathological processes, including nervous system embryogenesis,
225 regulation of immune system, cancer metastasis, bacterial and viral infection (31, 33-37). Sialic
226 acids are also important constituents of LOS and capsular polysaccharides of some bacterial
227 pathogens (38, 39); moreover, other bacterial pathogens not producing sialic acid, like some viruses
228 (40), are equipped with sialidases or neuraminidases, which have been shown to be key virulence
229 factors (41-44).

230 The crucial importance of sialic acids in the host-pathogen interplay is also well exemplified by
231 our knowledge on the function and genetic regulation of polysialic acid capsule and LOS decoration
232 with terminal sialic acid (Neu5Ac) in *N. meningitidis*. Most of the attention has been focused on the
233 role of surface-exposed sialic acids in mediating resistance to both phagocytosis and complement-
234 mediated killing via alternative pathway activation (10-16) resulting in enhanced meningococcal
235 survival in the intracellular environment (18-20), in the bloodstream, and in the CNS (17). In the
236 present study, we first aimed at validating the MM model by using a reference serogroup C strain
237 and its attenuated isogenic *cssA* knockout mutant unable to produce sialic acids. Then, comparison
238 of the virulence of the two strains was also instrumental to further explore the pathogenesis of MM
239 and subsequent cerebral damage by analyzing possible interaction between meningococcal surface-
240 exposed sialic acids and brain structures.

241 In this study, the inbred BALB/c mouse strain was used instead of the outbred CD-1 strain that
242 was originally employed to establish the MM model (27). Outbred mice present with larger genetic
243 variability that may be more suitable to uncover universal effects in a more diverse cohort and may
244 provide results more applicable to the human population (45, 46). However, such variability
245 requires larger sample sizes to reach sufficient statistical power and may hamper standardization
246 procedures, and targeted studies. In our case, the LD₅₀ of strain 93/4286 (without passage in mice)
247 in inbred BALB/c mice was 10⁴ cfu, while the LD₅₀ in outbred CD-1 animals was approximately
248 10⁷ cfu of mouse-passages bacteria (27). To this regard, it is noteworthy that BALB/c mice carry
249 the s (susceptibility) mutation in the solute carrier family 11a member 1-encoding gene (*Slc11a1*),
250 which truncates the encoded protein (also known as natural resistance-associated macrophage
251 protein 1, Nramp1) and increases susceptibility to infection with *Mycobacteria* spp. and *Salmonella*
252 spp. (47-51).

253 The key role of surface-exposed sialic acids in meningococcal pathogenesis was confirmed in the
254 present experimental MM model. The LD₅₀ of the wild type strain 93/4286 was about four orders of
255 magnitude lower than that of the 93/4286 Ω *cssA* mutant (Fig. 2). Compared to the wild type strain,
256 the ability of the mutant to replicate in the brain (Fig. 3A) and spread systemically was severely
257 impaired (Fig. 3B). Histological analysis and bacterial immunostaining on brain slices confirmed
258 higher disease severity with more pronounced inflammation, vasculitis and hemorrhages in mice
259 infected with the wild type strain compared to those challenged with the *cssA*-defective mutant (Fig.
260 4 and Fig. 6). The histopathological finding is reminiscent of cerebral infarction that in humans
261 represents a complication in about 25% of patients suffering from bacterial meningitis and in 9% of
262 MM cases (52). Interestingly, 80% of mice infected with the wild type strain 93/4286 presented
263 with severe inflammation in the *corpus callosum* (Fig. 4), and most of the immuno-positive signal
264 was localized in this brain structure by immunofluorescence with a meningococcal antiserum (Fig.
265 5). As expected, meningococci were also detected on the meninges, in the ventricles, and in the
266 choroid plexus. Massive presence of bacteria in the vessels as well as in the epithelium of the

267 choroid plexus and ventricular system is a very common finding in histopathological examination
268 of patients with MM (53, 54). Indeed, the choroid plexus is considered as an important gateway for
269 meningococcal traversal from the bloodstream into the CNS during meningitis in humans (55). It is
270 very likely that the bacteria utilize this highly vascularized site to spread systemically from the CNS
271 in the i.c. mouse model of MM, by using a reverse route. In contrast, the remarkable localization of
272 meningococci in the *corpus callosum* is unexpected, suggesting a certain tropism of *N. meningitidis*
273 for this brain structure. On a theoretical point of view, in order to accumulate within the *corpus*
274 *callosum*, in the i.c. mouse model of MM the bacteria have to leave the CSF space (since the CSF is
275 generated within the *plexus choroideus* and flows towards the subarachnoid space), survive in the
276 bloodstream, and re-enter into the brain. Our data seem to suggest the *corpus callosum* as a major
277 site of bacterial re-entry in the i.c. mouse model. This could be due to a high concentration of
278 adhesion molecules relevant to meningococcal-host cell interactions at the level of the cerebral
279 vessels or other structures in the *corpus callosum*.

280 Noteworthy, there is evidence in a murine model that heparan sulfate receptors (HSPGs), which
281 are targeted by meningococcal Opa, Opc and NhhA proteins (5) and mediate the interaction with
282 both epithelial and endothelial cells, are highly expressed in the *corpus callosum* (56). In addition, it
283 was also reported that the carcinoembryonic antigen-related cell-adhesion molecule-1 (CEACAM-
284 1), which serves as a receptor for several meningococcal Opa adhesins/invasins (5) are highly
285 expressed by oligodendrocytes, which are abundant in the *corpus callosum* (57). Furthermore, the
286 CEACAM-1 pathway activates matrix metalloproteinases that may be involved in blood-brain-
287 barrier breakdown (58). Noteworthy, oligodendrocytes specifically express the myelin-associated
288 glycoprotein (MAG), which is a member of the Siglec family of proteins (sialic acid-binding,
289 immunoglobulin-like lectins) capable of binding sialic acid (59). Thus, it is possible, although
290 speculative, that these molecular interactions could recruit the wild type meningococci and guide
291 they re-entry through the *corpus callosum*. In contrast, the absence of the *cssA*-defective mutant in
292 this brain structure might be due to both/either its inability to survive in the bloodstream as

293 demonstrated by its complete clearance after 48 h post infection in the peripheral organs (Fig. 3B),
294 and/or to the absence of surface-exposed sialic acid.

295 Although *corpus callosum* involvement as a complication of MM or invasive meningococcal
296 disease is reported to be a rare occurrence, a case of involvement of the *corpus callosum* with
297 cerebral ischemia and consequent callosal disconnection syndrome has been recently documented
298 by magnetic resonance imaging and diffusion tensor tractography (60). More recently, a case of a
299 reversible splenial lesion of the *corpus callosum* associated with MM has also been reported (61).
300 Whether the involvement of this brain structure in meningococcal meningitis/meningoencephalitis
301 as revealed by advanced imaging technologies may have actually been underestimated in the past, is
302 not clear yet. In fact, the histological evidence of the localization of meningococci in the *corpus*
303 *callosum* of patients who died of meningococcal disease does not yet exist. This limits our finding
304 to the analyzed meningococcal serogroup and strain, and to the i.c. mouse model of MM used in
305 this study.

306 The results of our study are consistent with the data reported by Vogel *et al.* (7) with a
307 bacteraemia model in infant rats with serogroup B *N. meningitidis* strain B1940 and a set of
308 isogenic mutants defective in either capsule synthesis or LOS sialylation. Infection of infant rats
309 with the wild type strain caused severe bacteremia, while an isogenic mutant strain defective in
310 capsule synthesis (but expressing a sialylated LOS) caused bacteremia only when a 10^6 cfu higher
311 bacterial dose was used. In addition, when infant rats were infected with encapsulated
312 meningococci that were unable to sialylate the LOS, bacteremia could never be induced, even with
313 an infective dose as high as 10^8 cfu, suggesting that both forms of sialic acid on the bacterial cell
314 surface are indispensable for systemic meningococcal survival in the infant rat model (7). Our study
315 further expands these data to CNS infection dynamics, having, however, in mind all the limitations
316 of an i.c. mouse model that exploits a non-natural infection route. Histological analysis and
317 bacterial immunostaining indicates surface-exposed sialic acid as a main determinant for
318 meningococcal intracellular growth/survival as reported before (18, 19) and also a possible

319 mediator in the interaction between meningococci and neuronal cells in the pathogenesis of invasive
320 meningococcal disease. Noteworthy, sialic acid-dependent interactions play a major role in
321 metastatic invasion of the *corpus callosum* by tumor cells. In humans, the frequency of polysialic
322 acid-positive cells and polysialyltransferase expression were higher in diffuse and recurrent
323 astrocytoma (associated with the invasion of the *corpus callosum*) than in astrocytoma with lower
324 spreading potential (62). This study suggests that tumor cells expressing polysialic acid on neural
325 cell adhesion molecules (NCAMs) may interact with adhesive receptors in the *corpus callosum*,
326 thus allowing tumor cell migration and localization in this brain structure (62). Similar molecular
327 interactions may explain the massive localization of wild type meningococci in the *corpus callosum*
328 in our MM model, proposing a new role of microbial surface-exposed sialic acids in the interplay
329 between *N. meningitidis* and the host in the pathogenesis of meningococcal disease that, however,
330 should be further explored.

331

332 MATERIALS AND METHODS

333 **Bacterial strains and growth conditions.** The meningococcal strains used in this study are the
334 serogroup C strain 93/4286 and the sialic acid deficient isogenic mutant 93/4286 Ω_{cssA} . The
335 93/4286 strain belonging to the ET-37 hypervirulent lineage (cc ST-11) was kindly provided by
336 Novartis Vaccine and Diagnostics, Siena, Italy. Meningococci were cultured on gonococcus (GC)
337 (Oxoid S.p.A., Milan, Italy) agar/broth supplemented with 1% (vol/vol) Polyvitox (Oxoid) at 37°C
338 with 5% CO₂. When needed, erythromycin (Sigma-Aldrich, Merck KGaA, Darmstadt, Germany)
339 was added to a final concentration of 7 $\mu\text{g ml}^{-1}$. Meningococci were also cultured in Dulbecco's
340 modified Eagle medium (DMEM) (Microgem, Naples, Italy) with 10% fetal bovine serum heat
341 inactivated (Microgem) and 2 mM L-glutamine (Microgem). To evaluate the fitness of each strain,
342 at every stage of growth, serial dilutions were plated on GC agar in the presence or absence of
343 erythromycin and incubated at 37°C with 5% CO₂ for 24 h. After growth, viable cell counts were
344 determined by the CFU method. The growth rate μ (h^{-1}) of the *cssA* mutant and the wild-type strain
345 was calculated as described by Barlow and coworkers (63), and the number of generation (G) and *t*
346 per generation were calculated as described by Gillespie and coworkers (64).

347 All experiments were performed in triplicate with three independent cultures, the results obtained
348 were analyzed and graphically reported by using GraphPad Prism (v.4) software, and statistical
349 significance was examined by the Student's *t*-test. Pairwise competition experiments were used to
350 estimate the *in vitro* fitness of *cssA* defective mutant relative to that of the wild type strain. Equal
351 numbers of CFU of the isogenic mutant and wild type strains were mixed together (1:1), and the
352 bacteria were allowed to grow together competitively in antibiotic-free GC broth at 37°C.
353 Experiments were conducted as previously described (65).

354 Inocula for mouse challenge were prepared by cultivating bacteria in GC broth until mid-
355 logarithmic phase. Viable cell counts were determined, and bacteria were frozen at -80°C with 10%
356 glycerol until use. *Escherichia coli* strain DH5 α was used in cloning procedures. This strain was

357 grown in Luria-Bertani (LB) (Oxoid) medium. To allow plasmid selection, LB medium was
358 supplemented with ampicillin (50 μ g ml⁻¹) (Sigma-Aldrich, Merck KGaA).

359

360 **DNA procedures, plasmids and transformation of *N. meningitidis*.** High-molecular-weight
361 genomic DNA from *N. meningitidis* strains was prepared as previously reported (66). DNA
362 fragments were isolated by using acrylamide slab gels and recovered by electroelution as described
363 before (67). Oligonucleotide synthesis and DNA sequencing were performed by Ceinge-Advanced
364 Biotechnologies, Naples, Italy. DNA sequence analysis was carried out by using the GeneJockey
365 Sequence Processor software (Biosoft) and multiple sequence alignment tool Clustal W
366 (<http://www.ebi.ac.uk/Tools/msa/clustalw2/>).

367 To construct the pDE Δ *cssA* vector, a genomic fragment of *cssA* [also known as *siaA*, *synA* or
368 *neuA* before proposal of a unified nomenclature for capsule loci (29)] (644 bp) was amplified from
369 genomic DNA of 93/4286 strain using the primers C_{ss}AXbaF (5'-
370 ATTGAACCTCTAGAGGTCATGATTCACGGCGACCG-3') and C_{ss}AXbaR (5'-
371 TGGCGTTCTAGAACATCAATTGAAGGGACACCG-3'). Amplification reactions were as
372 follows: 45 s of denaturation at 94°C, 45 s of annealing at 65°C, and 60 s of extension at 72°C for a
373 total of 30 cycles. Reactions were carried out in a MyCycler thermal cycler (Bio-Rad, Laboratories
374 S.r.l., Segrate, Milan, Italy). The amplicon was cloned into the *Xba*I site of *Neisseria-E. coli* shuttle
375 plasmid pDEX (66, 68). Plasmid pDE Δ *cssA* was then used to genetically inactivate by single cross-
376 over the *cssA* gene (NMC0054 or NMC_RS00310) of strain 93/4286 coding for the UDP-*N*-
377 acetylglucosamine 2-epimerase. Transformation experiments were performed using 0.1 to 1 μ g of
378 plasmid DNA as previously described (69). Transformants were selected on GC agar medium
379 supplemented with erythromycin. Gene disruption was demonstrated by Southern blot hybridization
380 using a 644-bp-long *cssA*-specific ³²P-labeled probe. Southern blot hybridizations were carried out
381 according to standard protocols (67). ³²P-labeling of DNA fragments was performed by random
382 priming using the Klenow fragment of *E. coli* DNA polymerase I and [α -³²P] dGTP (3,000 Ci

383 mmol⁻¹) (67). To detect capsular polysaccharide expression, a rabbit polyclonal antibody-coated
384 latex suspension against groups C and W135 *N. meningitidis* was used by latex slide agglutination
385 test (BD Directigen™ Meningitis Combo Test, BD Italia, Milan, Italy).

386

387 **Real-time RT-PCR experiments.** Semi-quantitative analysis of the *pile*, *fHbp*, *hrpA*, *nadA*, *opa54*,
388 *nhbA* transcript normalized to the level of expression of the *16S* rRNA gene (65) was performed by
389 real-time reverse transcriptase (RT)-PCR. Wild-type strain 93/4286 and *cssA* defective mutant were
390 grown to late logarithmic phase (OD₆₀₀, 1.0) in GC broth. Total bacterial RNAs were then extracted
391 by use of an RNeasy minikit (Qiagen, Venlo, the Netherlands) according to the manufacturer's
392 instructions. Before extraction, samples were treated with 2 volumes of RNA Protect Bacteria
393 reagent (Qiagen). DNA contamination was avoided by on-column treatment with an RNase-free
394 DNase set (Qiagen) according to the manufacturer's instructions. This procedure was performed in
395 triplicate for each strain. The concentration and integrity of the RNA samples were assessed by
396 measurement of the A₂₆₀/A₂₈₀ and A₂₆₀/A₂₃₀ ratios and were verified using a NanoDrop Lite
397 spectrophotometer (ThermoFisher Scientific, Waltham, Massachusetts, USA). Then, for each
398 sample, total RNAs (2γ) were reverse transcribed into cDNA as previously described (65). For
399 semiquantitative analysis, about 64-128 ng of each reverse transcription reaction mixture was used
400 to run a real-time PCR on an Applied Biosystems 7500 Fast Real-Time PCR System (Applied
401 Biosystems, Foster City, California, USA) with KiCqStart™ SYBR Green qPCR Ready Mix™,
402 Low ROX™ (Sigma-Aldrich) and with specific primers pair as reported in Supplemental Table S3.

403 PCR was conducted according to the manufacturer's guidelines as following reported: initial
404 holding and activation at 95°C for 10 min, PCR was performed for 40 cycles at 95°C for 20 s, 60°C
405 for 30 s and 72°C for 30 s. The post-PCR melt curve was performed between temperatures of 60°C
406 to 95°C with 1% temperature increments. Previously, standard curves were analyzed to determine
407 the efficiency of amplification and the 2^{-ΔΔCT} method was used for the analysis of the level (n-fold)
408 of change. Samples were run in the real-time PCR in triplicate, and statistical significance was

409 examined by Mann-Whitney U test. To quantify gene expression, we expressed the data as fold
410 change obtained using the $2^{-\Delta\Delta CT}$ method, where CT is threshold cycle.

411

412 **Mice, MM model and experimental design.** Eight-week-old female inbred BALB/c mice
413 weighing 19 to 20 g were purchased from Charles River Italia (Lecco, Italy). The mice were fed
414 with laboratory food pellets and tap water *ad libitum*, and were housed under specific pathogen free
415 conditions. All efforts were made to minimize animal suffering and reduce the number of mice in
416 accordance with the European Communities Council Directive of November 24, 1986
417 (86/609/EEC). The study was approved by the Ethical Animal Care and Use Committee (Prot.
418 number 2, 14 December 2012) and the Italian Ministry of Health (Prot. number 0000094-A-
419 03/01/2013). For brain histology and cerebral bleeding analysis, animal experiments were
420 performed at the Azienda Ospedaliera Universitaria Senese and authorised by the Local Ethics
421 Committee (Comitato Etico Locale, Azienda Ospedaliera Universitaria Senese, 21.05.2012) and the
422 Italian Ministry of Health (Document no. 131/2013, 30.05.2013).

423 Mice were infected by the i.cist. route as previously described (27, 30, 70). Bacteria for mouse
424 challenge were prepared as previously reported (27), thawed, centrifuged for 15 min at 1500 x g,
425 and suspended in GC broth with iron dextran (5 mg/kg; Sigma-Aldrich, Merck KGaA).
426 Approximately 2 h before infection, animals were injected intraperitoneally (i.p.) with iron dextran
427 (250 mg kg⁻¹). Animals were lightly anesthetized (50 mg/kg ketamine and 3 mg/kg xylazine or
428 Zoletil 20 [30 mg/kg; VirbacSrl] and Xilor [8 mg/kg; Bio 98 Srl]), and bacteria (suspended in a
429 total volume of 10 µl) were inoculated by hand-puncturing the *cisterna magna* of mice using a 30-
430 gauge needle (BD Italia, Milan, Italy). Mice were monitored for possible seizures due to
431 inoculation. Clinical signs were monitored according to a previously described coma scale (71), and
432 mice with a score of 2 were euthanized and recorded as dead for statistical analysis .

433 For brain histology and cerebral bleeding analysis, brains were removed and dissected into the
434 two hemispheres and cerebellum. One hemisphere was fixed in 4% paraformaldehyde (PFA) in

435 Phosphate-Buffered Saline (PBS) (w/v) for histological analysis, while the other one was frozen in
436 dry ice for assessment of intracerebral bleeding. Samples were not collected from animals found
437 dead or humanely sacrificed before 48 h.

438

439 **Animal survival and cfu counts.** Different bacterial doses ranging from 10^4 to 10^6 cfu per mouse
440 for the 93/4286 wild type strain, and from 10^7 to 10^9 for the 93/4286 Ω_{cssA} isogenic mutant were
441 used to inoculate animals (n=6/dose). Control mice were inoculated with GC broth. Every day
442 throughout the whole experiment, animals were monitored for clinical signs, and body weight and
443 temperature were measured as previously described (27). Survival was recorded for a week. To
444 determine the number of meningococci in the brain over time, animals were infected with 5×10^5
445 cfu/mouse and sacrificed at different time points (4, 24, 48, and 72 h) (n=3/time point) after
446 infection. To compare the virulence of the wild type strain versus the *cssA*-defective mutant, two
447 groups of mice (n=5/group) were infected with 5×10^5 cfu/mouse and sacrificed 48 h after challenge
448 for organ collection. Brain, spleen, and liver were excised and homogenized in 1 ml of GC medium.
449 Viable cell counts were performed by plating 10-fold dilutions onto GC agar plates with (mutant) or
450 without (wild type) erythromycin.

451

452 **Brain histology.** Experiments were performed with a total number of 20 mice, of which 8 were
453 infected with the wild type strain and 8 were challenged with the *cssA*-defective mutant, and four
454 served as control. Infection dose was 6×10^5 cfu/mouse. Brain hemispheres from mice infected for
455 48 hours were prepared for cryopreservation by incubation in 18% sucrose in PBS (w/v) at 4 °C
456 overnight. Hemispheres were mounted in OCT compound and cut coronally using a Leica 3050S
457 cryostat (Leica Biosystems, Wetzlar, Germany). Forty-five μ m-thick coronal sections were sampled
458 at a frequency of every 15th slice. Additional 10 μ m sections were obtained for immunofluorescence
459 analysis. Histopathological evaluations were made on sections stained with cresyl violet for Nissl
460 substance.

461

462 **Immunofluorescence.** Slices were incubated with a primary rabbit polyclonal antibody against
463 whole-cell preparation of serogroup A, B, and C *N. meningitidis* (ViroStat, cat. # 6122, Portland,
464 ME, USA) at a dilution of 1:1000. This antibody was reactive against both encapsulated and
465 unencapsulated meningococci (18, 19). Sections were washed three times with PBS and incubated
466 with the secondary antibody (goat anti-rabbit Cy3; Jackson, West Grove, PA, USA) for 45 min at
467 room temperature in the dark. Primary and secondary antibodies were diluted in Tris Buffered
468 Saline (TBS; Sigma-Aldrich, Merck KGaA) containing 0.5% bovine serum albumin. After washing,
469 slides were counterstained with DAPI for 1 min, washed and mounted with Mowiol[®] (Merck)
470 containing 2.5% Dabco[®] (Sigma-Aldrich, Merck KGaA). Pictures were obtained using a Zeiss
471 fluorescent microscope (AxioImager M1, Zeiss, West Germany) equipped with a digital camera
472 (AxioCamHRc). Overview pictures were created by combining photos obtained with a 10x
473 objective and mosaic reconstruction using the AxioVision 4.8 software (Zeiss, Oberkochen,
474 Germany).

475

476 **Analysis of cerebral bleeding.** Cerebral haemorrhages were assessed as previously described (72).
477 Briefly, brain hemispheres were cut in a frontal plane into 30 μ m-thick sections, and serial sections
478 were photographed with a digital camera at 0.3 mm-intervals. For each animal, 5 comparable brain
479 sections were analyzed. The bleeding spots were counted, and the relative areas of bleeding were
480 measured by using the UTHSCSA Image Tool (Texas, USA). Cumulative bleeding areas were
481 divided by the whole slice area and computed into a total bleeding area/whole slice area x 1000.

482

483 **Statistical analysis.** Bacterial counts in different organs and time-points were represented as mean
484 \pm SD of cfu numbers isolated from single mice. Differences in growth rates in *in vitro* experiments
485 and differences in bacterial loads between mice infected with the wild type strain or the mutant
486 were examined by the Student's *t*-test. Mouse survival was estimated by the Kaplan-Meier survival

487 analysis, and differences were compared using the log-rank test ($P<0.05$). Differences in expression
488 of surface adhesins by RT Real time PCR and differences in cerebral bleeding were evaluated using
489 the Mann-Whitney U test ($P<0.05$).

490

491 **Table 1. Competition assay of 93/4286Ω_{cssA} defective mutant strain with wild type strain.**

Mutant strain	No. of generations ^a		Cost per generation ^b	$D_{0-1.00D}$ ^{b,c}	Relative fitness (g _R /g _S) ^b
	g _S	g _R			
93/4286Ω _{cssA}	9.93 ± 0.68	10.77 ± 0.85	-0.058 ± 0.01	0.057 ± 0.01	1.08 ± 0.02

492 ^a The number of generations of the mutant strain (g_R) and of the wild-type strain (g_S) was calculated
493 as described by Gillespie and coworkers (64). The values are the means ± SD_s from four
494 independent experiments.

495 ^b The values are presented as the means ± SD_s from four independent experiments.

496 ^c The difference in fitness ($D_{0-1.00D}$) was estimated by direct competition against an equal number
497 of CFU of the mutant - wild-type strain.

498

499

500 **SUPPLEMENTAL MATERIAL**

501 SUPPLEMENTAL FILE 1, PDF file, 810KB

502

503 **ACKNOWLEDGMENTS**

504 This research was supported in part by PRIN 2012 [grant number 2012WJSX8K]: “Host-microbe
505 interaction models in mucosal infections: development of novel therapeutic strategies”. We thanks
506 Robert Lukesch for excellent technical assistance, and Tiziana Braccini for excellent technical
507 assistance in *in vivo* experiments.

508

509 **REFERENCE**

- 510 1. van Deuren M, Brandtzaeg P, van der Meer JW. 2000. Update on meningococcal disease
511 with emphasis on pathogenesis and clinical management. Clin Microbiol Rev 13:144-166.
512
- 513 2. Plant L, Jonsson AB. 2003. Contacting the host: insights and implications of pathogenic
514 *Neisseria* cell interactions. Scand J Infect Dis 35:608-613.
515
- 516 3. Schryvers AB, Stojiljkovic I. 1999. Iron acquisition systems in the pathogenic *Neisseria*.
517 Mol Microbiol 32:1117-1123.
518
- 519 4. Virji M, Makepeace K, Ferguson DJ, Watt SM. 1996. Carcinoembryonic antigens (CD66)
520 on epithelial cells and neutrophils are receptors for Opa proteins of pathogenic neisseriae.
521 Mol Microbiol 22:941-950.
522
- 523 5. Hill DJ, Griffiths NJ, Borodina E, Virji M. 2010. Cellular and molecular biology of
524 *Neisseria meningitidis* colonization and invasive disease. ClinSci (Lond) 118:547-564.
525
- 526 6. Tzeng YL, Thomas J, Stephens DS. Regulation of capsule in *Neisseria meningitidis*. 2015.
527 Crit Rev Microbiol 19:1-14.
528
- 529 7. Vogel U, Hammerschmidt S, Frosch M. 1996. Sialic acids of both the capsule and the
530 sialylated lipooligosaccharide of *Neisseria meningitis* serogroup B are prerequisites for
531 virulence of meningococci in the infant rat. Med Microbiol Immunol 185:81-87.
532
- 533 8. Stefanelli P, Miglietta A, Pezzotti P, Fazio C, Neri A, Vacca P, Voller F, D'Ancona FP,
534 Guerra R, Iannazzo S, Pompa MG, Rezza G. 2016. Increased incidence of invasive

meningococcal disease of serogroup C / clonal complex 11, Tuscany, Italy, 2015 to 2016.
Euro Surveill 21:(12).

537

9. Mandrell RE, Kim JJ, John CM, Gibson BW, Sugai JV, Apicella MA, Griffiss JM,
Yamasaki R. 1991. Endogenous sialylation of the lipooligosaccharides of *Neisseria*
meningitidis. J Bacteriol 173:2823-2832.

541

10. Estabrook MM, Christopher NC, Griffiss JM, Baker CJ, Mandrell RE. 1992. Degree of
endogenous LOS sialylation and amount of sialic acid capsule were associated with each
other and with susceptibility to killing by neutrophils for the non-2b:P1.2 strains. J Infect
Dis 166:1079-1088.

546

11. Estabrook MM, Griffiss JM, Jarvis GA. 1997. Sialylation of *Neisseria meningitidis*
lipooligosaccharide inhibits serum bactericidal activity by masking lacto-N-neotetraose.
Infect Immun 65:4436-4444.

550

12. Hammerschmidt S, Birkholz C, Zähringer U, Robertson BD, van Putten J, Ebeling O,
Frosch M. 1994. Contribution of genes from the capsule gene complex (*cps*) to
lipooligosaccharide biosynthesis and serum resistance in *Neisseria meningitidis*. Mol
Microbiol 11:885-896.

555

13. Jarvis GA. 1995. Recognition and control of neisserial infection by antibody and
complement. Trends Microbiol 3:198-201.

558

- 559 14. John CM, Phillips NJ, Din R, Liu M, Rosenqvist E, Høiby EA, Stein DC, Jarvis GA. 2016.
560 Lipooligosaccharide structures of invasive and carrier isolates of *Neisseria meningitidis* are
561 correlated with pathogenicity and carriage. J Biol Chem 291:3224-3238.
562
- 563 15. Lewis LA, Carter M, Ram S. 2012. The relative roles of factor H binding protein, neisserial
564 surface protein A, and lipooligosaccharide sialylation in regulation of the alternative
565 pathway of complement on meningococci. J Immunol 188:5063-5072.
566
- 567 16. Ram S, Mackinnon FG, Gulati S, McQuillen DP, Vogel U, Frosch M, Elkins C, Guttormsen
568 HK, Wetzler LM, Oppermann M, Pangburn MK, Rice PA. 1999. The contrasting
569 mechanisms of serum resistance of *Neisseria gonorrhoeae* and group B *Neisseria*
570 *meningitidis*. Mol Immunol 36:915-928.
571
- 572 17. Stephens DS. 2009. Biology and pathogenesis of the evolutionarily successful,obligate
573 human bacterium *Neisseria meningitidis*. Vaccine 27 Suppl 2 :B71-7.
574
- 575 18. Spinoso MR, Progida C, Tala A, Cogli L, Alifano P, Bucci C. 2007. The *Neisseria*
576 *meningitidis* capsule is important for intracellular survival in human cells. Infect Immun
577 75:3594-3603.
578
- 579 19. Talà A, Cogli L, De Stefano M, Cammarota M, Spinoso MR, Bucci C, Alifano P. 2014.
580 Serogroup-specific interaction of *Neisseria meningitidis* capsular polysaccharide with host
581 cell microtubules and effects on tubulin polymerization. Infect Immun 82(1):265-274.
582

- 583 20. Jones A, Georg M, Maudsdotter L, Jonsson AB. 2009. Endotoxin, capsule, and bacterial
584 attachment contribute to *Neisseria meningitidis* resistance to the human antimicrobial
585 peptide LL-37. J Bacteriol 191:3861-3868.
- 586
- 587 21. Hammerschmidt S, Müller A, Sillmann H, Mühlenhoff M, Borrow R, Fox A, van Putten J,
588 Zollinger WD, Gerardy-Schahn R, Frosch M. 1996a. Capsule phase variation in *Neisseria*
589 *meningitidis* serogroup B by slipped-strand mispairing in the polysialyltransferase gene
590 (*siaD*): correlation with bacterial invasion and the outbreak of meningococcal disease. Mol
591 Microbiol 20:1211-1220.
- 592
- 593 22. Hammerschmidt S, Hilse R, van Putten JP, Gerardy-Schahn R, Unkmeir A, Frosch M.
594 1996b. Modulation of cell surface sialic acid expression in *Neisseria meningitidis* via a
595 transposable genetic element. EMBO J 15:192-198.
- 596
- 597 23. Unkmeir A, Kämmerer U, Stade A, Hübner C, Haller S, Kolb-Mäurer A, Frosch M, Dietrich
598 G. 2002. Lipooligosaccharide and polysaccharide capsule: virulence factors of *Neisseria*
599 *meningitidis* that determine meningococcal interaction with human dendritic cells. Infect
600 Immun 70:2454-2462.
- 601
- 602 24. Weber MV, Claus H, Maiden MC, Frosch M, Vogel U. 2006. Genetic mechanisms for loss
603 of encapsulation in polysialyltransferase-gene-positive meningococci isolated from healthy
604 carriers. Int J Med Microbiol 296:475-484.
- 605
- 606 25. Deghmane AE, Giorgini D, Larribe M, Alonso JM, Taha MK. 2002. Down-regulation of pili
607 and capsule of *Neisseria meningitidis* upon contact with epithelial cells is mediated by CrgA
608 regulatory protein. Mol Microbiol 43:1555-1564.

609

610 26. Bartley SN, Tzeng YL, Heel K, Lee CW, Mowlaboccus S, Seemann T, Lu W, Lin YH,
611 Ryan CS, Peacock C, Stephens DS, Davies JK, Kahler CM. 2013. Attachment and invasion
612 of *Neisseria meningitidis* to host cells is related to surface hydrophobicity, bacterial cell size
613 and capsule. PLoS One 8(2):e55798.

614

615 27. Colicchio R, Ricci S, Lamberti F, Pagliarulo C, Pagliuca C, Braione V, Braccini T, Talà A,
616 Montanaro D, Tripodi S, Cintonino M, Troncone G, Bucci C, Pozzi G, Bruni CB, Alifano P,
617 Salvatore P. 2009. The meningococcal ABC-Type L-glutamate transporter GltT is necessary
618 for the development of experimental meningitis in mice. Infect Immun 77:3578-3587.

619

620 28. Murkin AS, Chou WK, Wakarchuk WW, Tanner ME. 2004. Identification and mechanism
621 of a bacterial hydrolyzing UDP-N-acetylglucosamine 2-epimerase. Biochemistry 43:14290-
622 14298.

623

624 29. Harrison OB, Claus H, Jiang Y, Bennett JS, Bratcher HB, Jolley KA, Corton C, Care R,
625 Poolman JT, Zollinger WD, Frasch CE, Stephens DS, Feavers I, Frosch M, Parkhill J, Vogel
626 U, Quail MA, Bentley SD, Maiden MC. 2013. Description and nomenclature of *Neisseria*
627 *meningitidis* capsule locus. Emerg Infect Dis 19:566-573.

628

629 30. Ricci S, Grandgirard D, Wenzel M, Braccini T, Salvatore P, Oggioni MR, Leib SL, Koedel
630 U. 2014. Inhibition of matrix metalloproteinases attenuates brain damage in experimental
631 meningococcal meningitis. BMC Infect Dis 14:726.

632

633 31. Chen X, Varki A. 2010. Advances in the biology and chemistry of sialic acids. ACS Chem
634 Biol 5:163-176.

635

636

637

638

639

640

641

642

643

644

645

646

647

648

649

650

651

652

653

654

655

656

657

658

659

660

32. Varki NM, Strobert E, Dick EJ Jr, Benirschke K, Varki A. 2011. Biomedical differences between human and nonhuman hominids: potential roles for uniquely human aspects of sialic acid biology. *Annu Rev Pathol* 6:365-393.

33. Angata T, Varki A. 2002. Chemical diversity in the sialic acids and related alpha-keto acids: an evolutionary perspective. *Chem Rev* 102:439-469.

34. Chen GY, Chen X, King S, Cavassani KA, Cheng J, Zheng X, Cao H, Yu H, Qu J, Fang D, Wu W, Bai XF, Liu JQ, Woodiga SA, Chen C, Sun L, Hogaboam CM, Kunkel SL, Zheng P, Liu Y. 2011. Amelioration of sepsis by inhibiting sialidase-mediated disruption of the CD24-SiglecG interaction. *Nat Biotechnol* 29:428-435.

35. Li Y, Chen X. 2012. Sialic acid metabolism and sialyltransferases: natural functions and applications. *Appl Microbiol Biotechnol* 94:887-905.

36. Chang YC, Nizet V. 2014. The interplay between Siglecs and sialylated pathogens. *Glycobiology*. 24:818-825.

37. Petridis AK, El-Maarouf A, Rutishauser U. 2004. Polysialic acid regulates cell contact-dependent neuronal differentiation of progenitor cells from the subventricular zone. *Dev Dyn* 230:675-684.

38. Severi E, Hood DW, Thomas GH. 2007. Sialic acid utilization by bacterial pathogens. *Microbiology* 153:2817-2822.

- 661 39. Vimr ER, Kalivoda KA, Deszo EL, Steenbergen SM. 2004. Diversity of microbial sialic
662 acid metabolism. *Microbiol Mol Biol Rev* 68:132-153.
663
- 664 40. Suzuki Y. 2005. Sialobiology of influenza: molecular mechanism of host range variation of
665 influenza viruses. *Biol Pharm Bull* 28:399-408.
666
- 667 41. Amano A, Chen C, Honma K, Li C, Settem RP, Sharma A. 2014. Genetic characteristics
668 and pathogenic mechanisms of periodontal pathogens. *Adv Dent Res* 26:15-22.
669
- 670 42. Camara M, Boulnois GJ, Andrew PW, Mitchell TJ. 1994. A neuraminidase from
671 *Streptococcus pneumoniae* has the feature of a surface protein. *Infect Immun* 62:3688-3695.
672
- 673 43. Gualdi L, Hayre JK, Gerlini A, Bidossi A, Colomba L, Trappetti C, Pozzi G, Docquier JD,
674 Andrew P, Ricci S, Oggioni MR. 2012. Regulation of neuraminidase expression in
675 *Streptococcus pneumoniae*. *BMC Microbiol* 12:200.
676
- 677 44. Juge N, Tailford L, Owen CD. 2016. Sialidases from gut bacteria: a mini-review. *Biochem*
678 *Soc Trans* 44:166-175.
679
- 680 45. Festing MFW. 1976. Phenotypic variability of inbred and outbred mice. *Nature* 263:230-
681 232.
682
- 683 46. Festing MFW. 1999. Warning: the use of heterogeneous mice may seriously damage your
684 research. *Neurobiol Aging* 20: 237-244.
685

- 686 47. Medina E, North RJ. 1996a. Evidence inconsistent with a role for the *Bcg* gene (*Nramp1*) in
687 resistance of mice to infection with virulent *Mycobacterium tuberculosis*. *J Exp Med*
688 183:1045-1051.
- 689
- 690 48. Medina E, North RJ. 1996b. Mice that carry the resistance allele of the *Bcg* gene (*Bcgr*)
691 develop a superior capacity to stabilize bacilli Calmette-Guerin (BCG) infection in their
692 lungs and spleen over a protracted period in the absence of specific immunity. *Clin Exp*
693 *Immunol* 104:44-47.
- 694
- 695 49. Medina E, North RJ. 1999. Genetically susceptible mice remain proportionally more
696 susceptible to tuberculosis after vaccination. *Immunology* 96:16-21.
- 697
- 698 50. Vidal SM, Malo D, Vogan K, Vogan K, Skamene E, Gros P. 1993. Natural resistance to
699 infection with intracellular parasites: isolation of a candidate for *Bcg*. *Cell* 73:469-485.
- 700
- 701 51. Vidal S, Tremblay ML, Govoni G, Gauthier S, Sebastiani G, Malo D, Skamene E, Olivier
702 M, Jothy S, Gros P. 1995. The *Iti/Lsh/Bcg* locus: natural resistance to infection with
703 intracellular parasites is abrogated by disruption of the *Nramp1* gene. *J Exp Med* 182:655-
704 666.
- 705
- 706 52. Schut ES, Lucas MJ, Brouwer MC, Vergouwen MD, van der Ende A, van de Beek D. 2012.
707 Cerebral infarction in adults with bacterial meningitis. *Neurocrit Care* 16:421-427.
- 708
- 709 53. Guarner J, Greer PW, Whitney A, Shieh WJ, Fischer M, White EH, Carlone GM, Stephens
710 DS, Popovic T, Zaki SR. 2004. Pathogenesis and diagnosis of human meningococcal
711 disease using immunohistochemical and PCR assays. *Am J Clin Pathol* 122:754-764.

712

713 54. Pron B, Taha MK, Rambaud C, Fournet JC, Pattey N, Monnet JP, Musilek M, Beretti JL,
714 Nassif X. 1997. Interaction of *Neisseria meningitidis* with the components of the blood-
715 brain barrier correlates with an increased expression of Pili. J Infect Dis 176:1285-1292.

716

717 55. Schwert C, Tenenbaum T, Kim KS, Schroten H. 2015. The choroid plexus-a multi-role
718 player during infectious diseases of the CNS. Front Cell Neurosci 9:80.

719

720 56. Kaur C, Sivakumar V, Yip GW, Ling EA. 2009. Expression of syndecan-2 in the amoeboid
721 microglial cells and its involvement in inflammation in the hypoxic developing brain. Glia.
722 57(3):336-49.

723

724 57. Neyazi B, Herz A, Stein KP, Gawish I, Hartmann C, Wilkens L, Erguen S, Dumitru CA,
725 Sandalcioğlu IE. 2017. Brain arteriovenous malformations: implications of CEACAM1-
726 positive inflammatory cells and sex on hemorrhage. Neurosurg Rev. 40(1):129-134.

727

728 58. Ludwig P, Sedláček J, Gelderblom M, Bernreuther C, Korkusuz Y, Wagener C, Gerloff C,
729 Fiehler J, Magnus T, Horst AK. 2013. Carcinoembryonic antigen-related cell adhesion
730 molecule 1 inhibits MMP-9-mediated blood-brain-barrier breakdown in a mouse model for
731 ischemic stroke. Circ Res 113:1013-1022

732

733 59. Huang JY, Wang YX, Gu WL, Fu SL, Li Y, Huang LD, Zhao Z, Hang Q, Zhu HQ, Lu PH.
734 2012. Expression and function of myelin-associated proteins and their common receptor
735 NgR on oligodendrocyte progenitor cells. Brain Res 1437:1-15.

736

- 737 60. Marchi NA, Ptak R, Wetzel C, Vargas MI, Schnider A, Nicastro N. 2016. Callosal
738 disconnection syndrome after ischemic stroke of the corpus callosum due to meningococcal
739 meningitis: A case report. *J Neurol Sci* 369:119-120.
- 740
- 741 61. Hayashi Y, Yasunishi M, Hayashi M, Asano T, Kimura A, Inuzuka T. 2017. Reversible
742 splenial lesion of the corpus callosum associated with meningococcal meningitis. *J Neurol*
743 *Sci* 373:81-82.
- 744
- 745 62. Suzuki M, Suzuki M, Nakayama J, Suzuki A, Angata K, Chen S, Sakai K, Hagihara K,
746 Yamaguchi Y, Fukuda M. 2005. Polysialic acid facilitates tumor invasion by glioma cells.
747 *Glycobiology* 15:887-894.
- 748
- 749 63. Hall BG, Acar H, Nandipati A, Barlow M. 2014. Growth rates made easy. *Mol Biol Evol.*
750 31(1):232-8.
- 751
- 752 64. Billington OJ, McHugh TD, Gillespie SH. 1999. Physiological cost of rifampin resistance
753 induced in vitro in *Mycobacterium tuberculosis*. *Antimicrob Agents Chemother.*
754 43(8):1866-9.
- 755
- 756 65. Colicchio R, Pagliuca C, Pastore G, Cicatiello AG, Pagliarulo C, Talà A, Scaglione E,
757 Sammartino JC, Bucci C, Alifano P, Salvatore P. 2015. Fitness Cost of Rifampin Resistance
758 in *Neisseria meningitidis*: In Vitro Study of Mechanisms Associated with rpoB H553Y
759 Mutation. *Antimicrob Agents Chemother.* 59(12):7637-49.
- 760

- 761 66. Bucci C, Lavitola A, Salvatore P, Del Giudice L, Massardo DR, Bruni CB, Alifano P. 1999.
762 Hypermutation in pathogenic bacteria: frequent phase variation in meningococci is a
763 phenotypic trait of a specialized mutator biotype. *Mol Cell* 3:435-445.
764
- 765 67. Sambrook J, Russell, DW. 2001. *Molecular cloning: a laboratory manual*, 3rd ed. Cold
766 Spring Harbor Laboratory Press, Cold Spring Harbor, NY.
767
- 768 68. Pagliarulo C, Salvatore P, De Vitis LR, Colicchio R, Monaco C, Tredici M, Talà A, Bardaro
769 M, Lavitola A, Bruni CB, Alifano P. 2004. Regulation and differential expression of *gdhA*
770 encoding NADP-specific glutamate dehydrogenase in *Neisseria meningitidis* clinical
771 isolates. *Mol Microbiol* 51:1757-1772.
772
- 773 69. Frosch M, Schultz E, Glenn-Calvo E, Meyer TF. 1990. Generation of capsule-deficient
774 *Neisseria meningitidis* strains by homologous recombination. *Mol Microbiol* 4:1215-1218.
775
- 776 70. Koedel U, Paul R, Winkler F, Kastenbauer S, Huang PL, Pfister HW. 2001. Lack of
777 endothelial nitric oxide synthase aggravates murine pneumococcal meningitis. *J*
778 *Neuropathol Exp Neurol* 60:1041-1050.
779
- 780 71. Liechti FD, Grandgirard D, Leppert D, Leib SL. 2014. Matrix metalloproteinase inhibition
781 lowers mortality and brain injury in experimental pneumococcal meningitis. *Infect Immun*
782 82:1710-1718.
783
- 784 72. Koedel U, Frankenberg T, Kirschnek S, Obermaier B, Häcker H, Paul R, Häcker G. 2009.
785 Apoptosis is essential for neutrophil functional shutdown and determines tissue damage in
786 experimental pneumococcal meningitis. *PLoS Pathog* 5:e1000461.

787 **Figure Legends**

788 **FIG 1.** Knock out of the *cssA* gene in the 93/4286 strain. Experimental design for *cssA* disruption
789 by single crossing-over (A). The genetic map of the *cps* locus Region A (capsule synthesis) of *N.*
790 *meningitidis* serogroup C was constructed on the basis of the available nucleotide sequences of
791 FAM18 (ET-37) in the NCBI data bank (https://www.ncbi.nlm.nih.gov/nuccore/NC_008767) with
792 arrows depicting gene orientation. The genetic determinants of plasmid pDE Δ *cssA* are: i) a DNA
793 fragment containing a DUS, required for efficient DNA uptake during transformation; ii) *ermC*, the
794 erythromycin resistance gene used as a selective marker for transformation; iii) Δ *cssA*, a 644 bp
795 *Xba*I DNA fragment spanning the central part of *cssA* and iv) black box, that indicates the plasmid
796 polylinker region. The physical map of the pDE Δ *cssA* plasmid is also indicated. Southern blot
797 analysis demonstrating inactivation of *cssA* (B). Chromosomal DNA was extracted from the
798 parental strains 93/4286 (lane 1) and an isogenic mutant, 93/4286 Ω *cssA* (lane 2), obtained by
799 transformation with pDE Δ *cssA* and selection with erythromycin. Chromosomal DNA was analyzed
800 by Southern blot using a *cssA*-specific probe. Bars on the right indicate *cssA*-specific fragments
801 whose sizes were deduced on the basis of the relative migration pattern of DNA ladders (bars on the
802 left).

803
804 **FIG 2.** Survival of mice infected with wild type or *cssA*-defective *N. meningitidis* strains. Three
805 groups of BALB/c mice (n= 6/dose) were infected i.cist. with 10^4 , 10^5 , and 10^6 cfu per mouse of the
806 wild type strain 93/4286 (A) and with 10^7 , 10^8 , and 10^9 cfu per mouse of the *cssA*-defective mutant
807 (B). Mice were monitored for a week, and survival was recorded. Results are expressed as percent
808 survival at different doses over time, the log rank p value was < 0.05 for mice infected with the wild
809 type strain.

810
811 **FIG 3.** Bacterial loads over time in mice inoculated with the 93/4286 or 93/4286 Ω *cssA* strains.
812 Time course of bacterial loads in the brain following i.cist. infection (A). Two groups of BALB/c

813 mice (n=20/group) were infected by the i.cist. route with 5×10^5 cfu of either the wild type strain
814 93/4286 or the *cssA*-defective mutant. Animals were sacrificed 4, 24, 48, and 72 h after infection
815 (3/time point). Brains were collected, homogenized in GC medium, and viable counts were
816 determined. Results are expressed as mean \pm SD log of cfu numbers per organ at different time
817 points after inoculation. Asterisks indicate statistical significance (**, $P < 0.01$). Bacterial loads over
818 time in spleen and liver (B). Two groups of BALB/c mice (n=5/group) were infected i.cist. with
819 2×10^6 cfu of either the wild type strain 93/4286 or the *cssA*-defective mutant. Animals were
820 sacrificed 48 h after infection. Spleens and livers were collected, homogenized, and viable counts
821 were determined. Results are expressed as log cfu numbers per organ. Horizontal bars indicate
822 mean logs of bacterial titers. Each symbol represents a single animal. Asterisks indicate statistical
823 significance (***, $P < 0.001$).

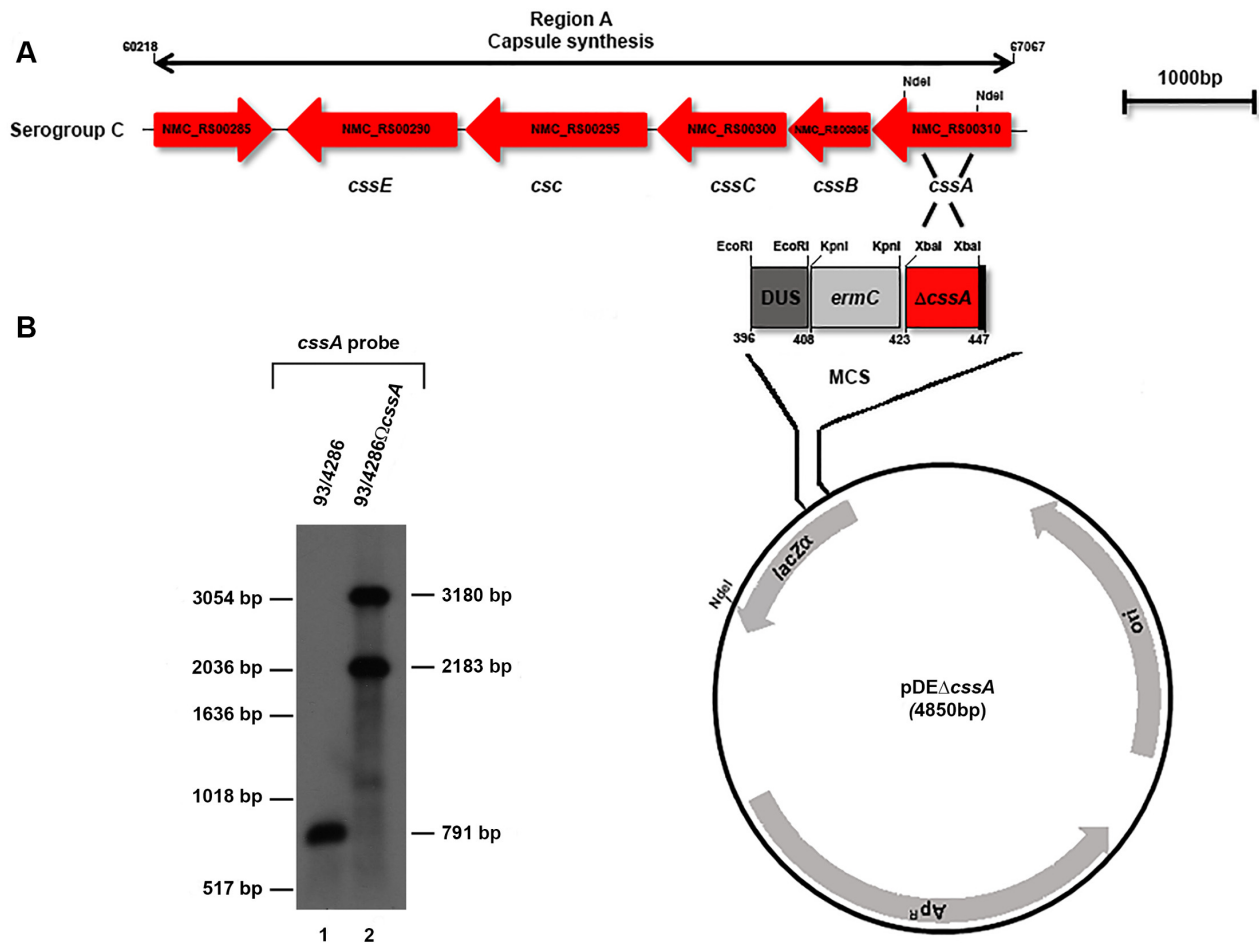
824

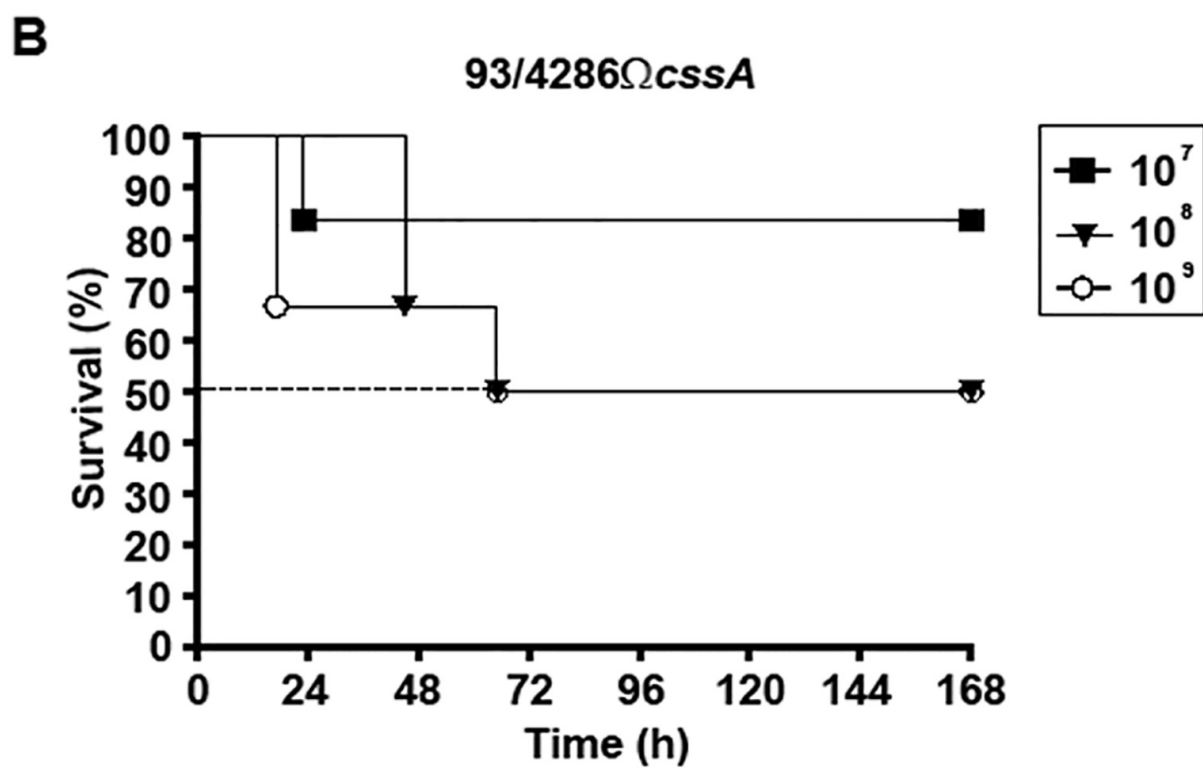
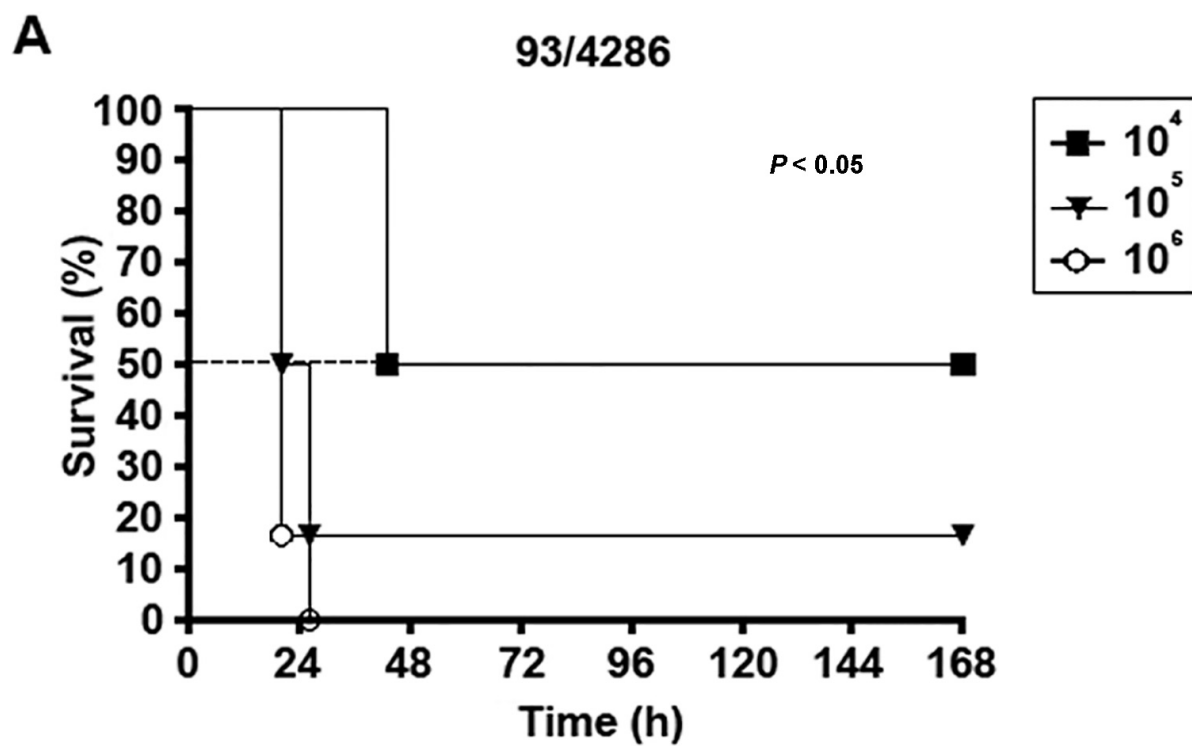
825 **FIG 4.** Cresyl violet stained sections of brains from animals mice infected with wild type or *cssA*-
826 defective *N. meningitidis* strains. BALB/c mice were challenged by the i.cist. route with either the
827 wild type 93/4286 or the mutant 93/4286 Δ *cssA* strains. At 48 h, brains were harvested and treated
828 for histological analysis. Forty-five μ m coronal sections were stained with cresyl violet. Overview
829 (mosaic reconstruction from 10x individual pictures) of the hippocampal region of a representative
830 animal infected with 93/4286 (A) or 93/4286 Δ *cssA* (B). Overview (objective 20x) of the meninges
831 (black arrowheads) and an inflamed penetrating vessel (white arrowheads) in an animal infected
832 with 93/4286 (C). Close up view (objective 40x) of the ventricular space of the animal infected with
833 93/4286 showing inflammatory cells (white arrowheads) and possible intraventricular haemorrhage
834 (black star) (D). Close up views (objective 40x) of the *corpus callosum* of animals infected with
835 93/4286 (E) or 93/4286 Δ *cssA*, with the presence of infiltrated inflammatory cells (white
836 arrowheads) (F).

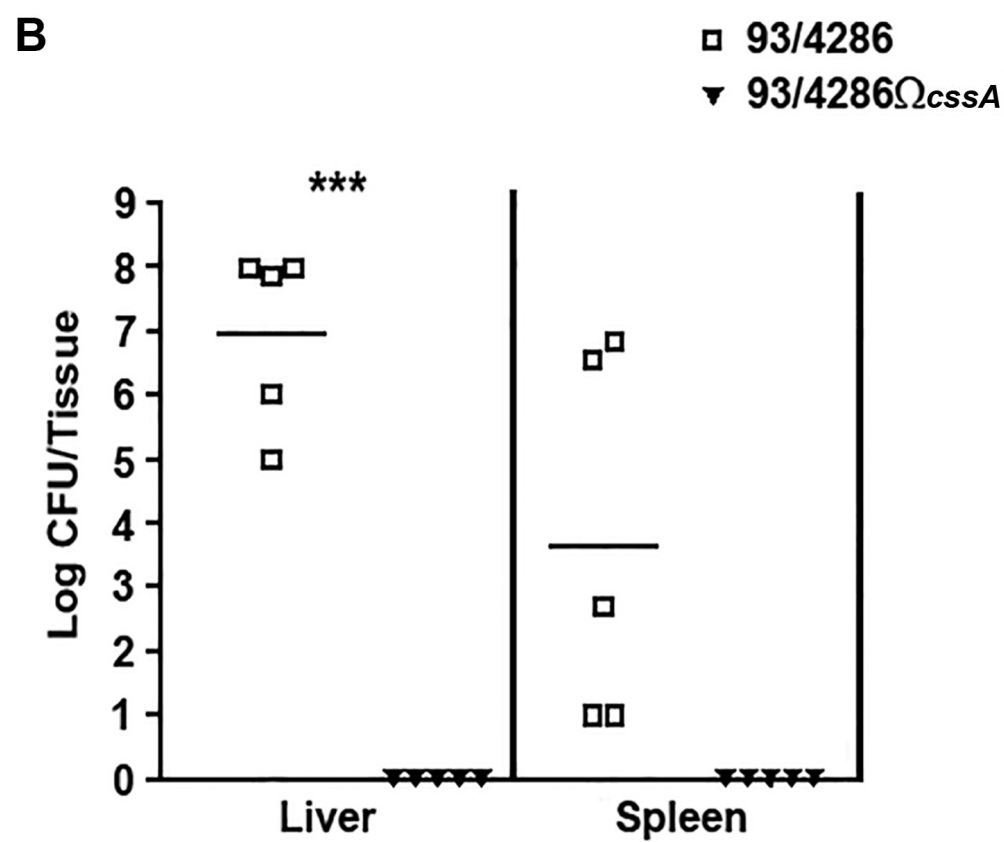
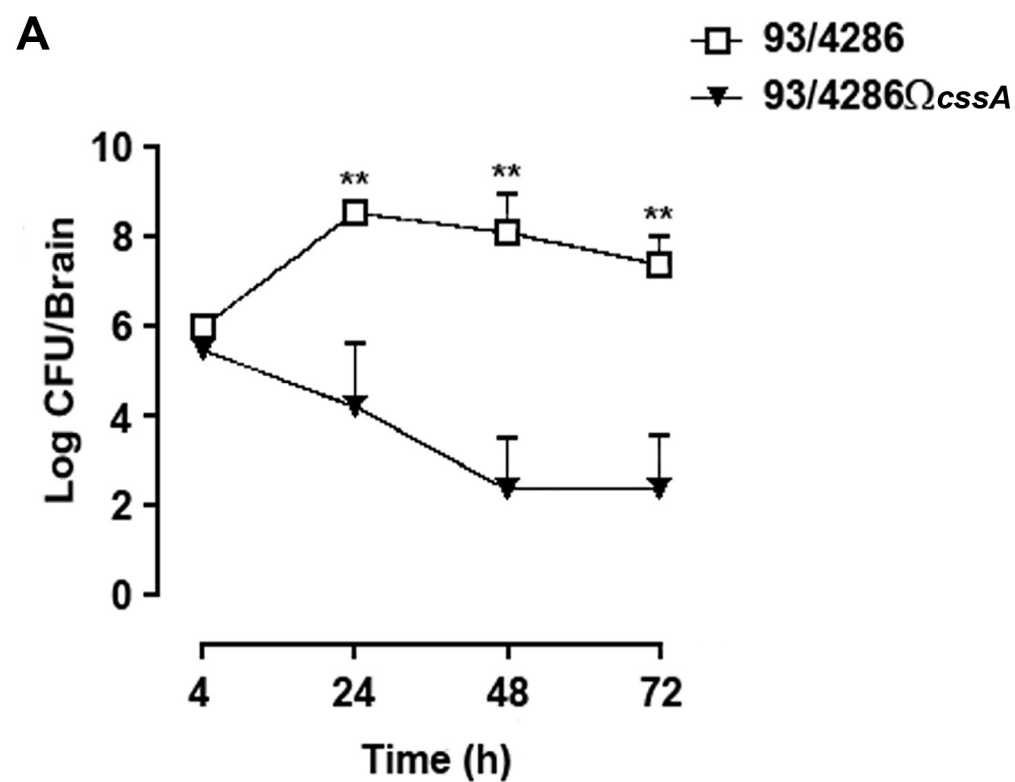
837

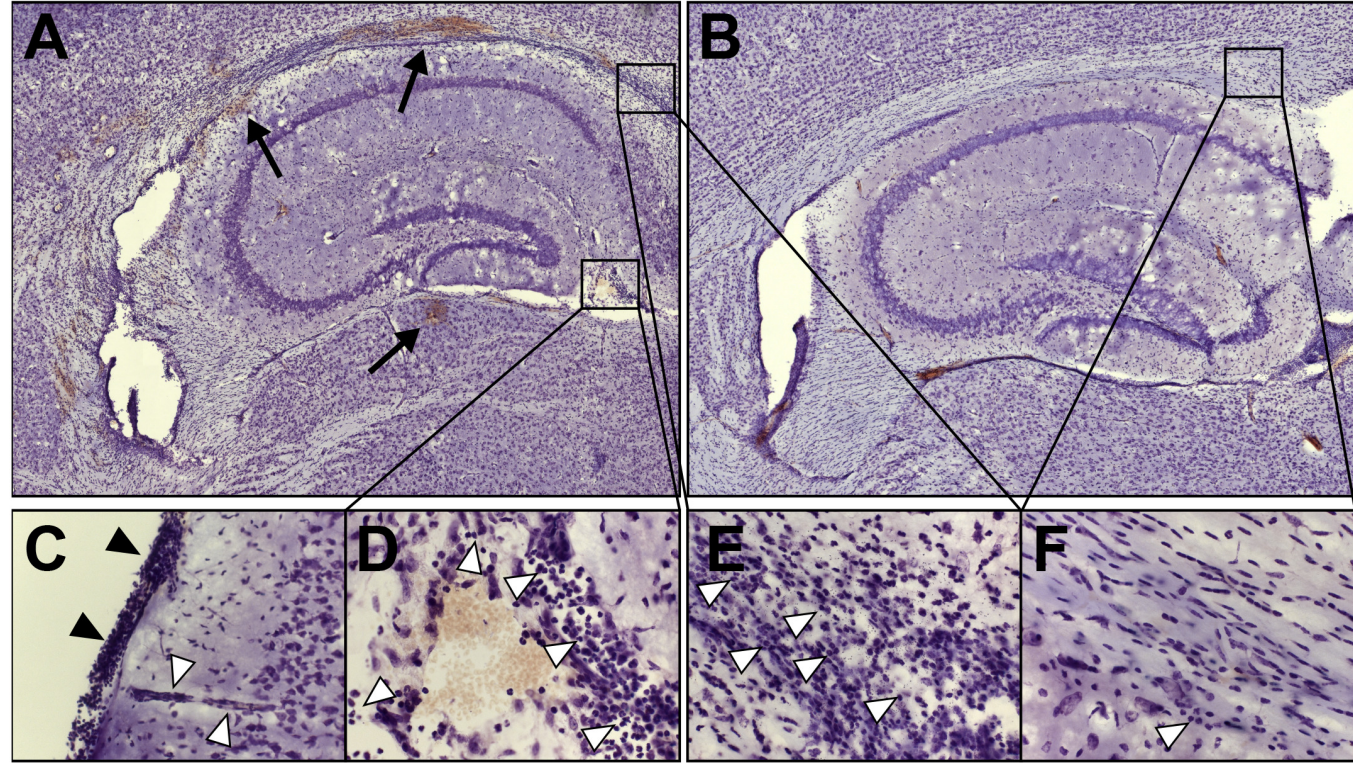
838 **FIG 5.** Immunofluorescence analysis of brain sections of mice infected with wild type 93/4286 or
839 mutant 93/4286 Ω cssA strains. Mice were infected and sacrificed as described in Fig. 4. Ten μ m
840 brain sections were treated with a rabbit meningococcal antiserum and then a goat anti-rabbit Cy3
841 serum. Slides were counterstained with DAPI and observed using a Zeiss fluorescence microscope.
842 Overview of the hippocampal region of two representative animals infected with either the wild
843 type 93/4286 (A-C) or the mutant 93/4286 Ω cssA (D-F) strains. In the insets (20X), *corpus callosum*
844 (B, E) and ventricles (C, F) from the brain of mice challenged with 93/4286 (B, C) or
845 93/4286 Ω cssA (E, F). Large quantities of bacteria are detected in samples from mice infected with
846 the wild type strain. In red, *N. meningitidis* immunostained with meningococcal antiserum. In blue,
847 DAPI.

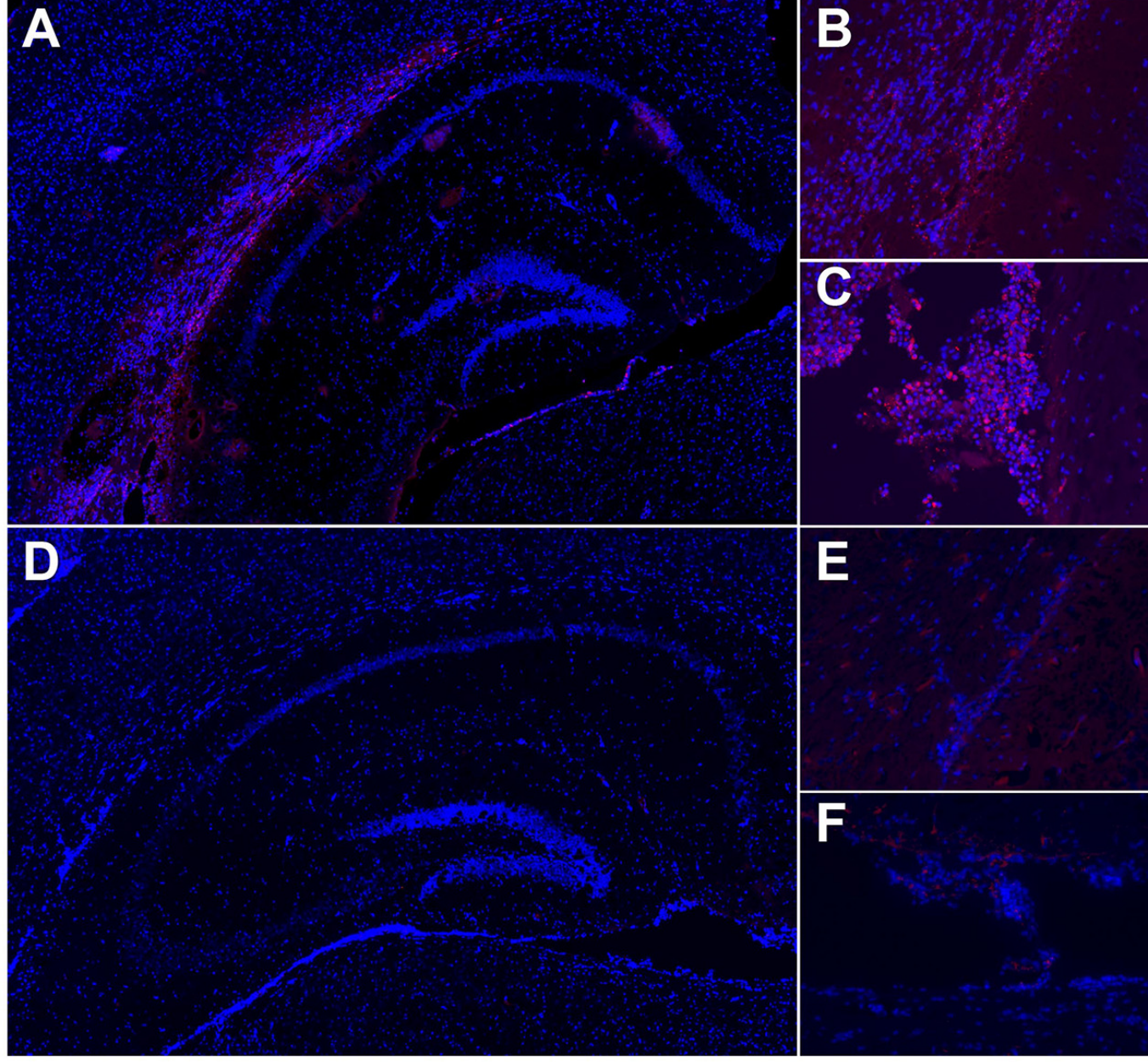
848
849 **FIG 6.** Cerebral bleeding in mice infected with 93/4286 or 93/4286 Ω cssA strains. BALB/c mice
850 were infected with either the wild type strain 93/4286 (n=8) or the mutant strain 93/4286 Ω cssA
851 (n=8) and sacrificed at 48 h. Brains were collected and immediately frozen in dry ice. Hemispheres
852 were cut in 30 μ m cryosections and photographed to determine the number of hemorrhagic spots
853 and the areas of bleeding. Macroscopical assessment of cerebral haemorrhages in animals
854 challenged with the wild type or the mutant strain (A). Enumeration of bleeding spots (B) and
855 measurement of hemorrhagic areas (C) were carried out on 5 comparable brain sections/mouse.
856 Data are represented as mean \pm SD. Differences were assessed by the Mann-Whitney test (*,
857 $P < 0.05$).







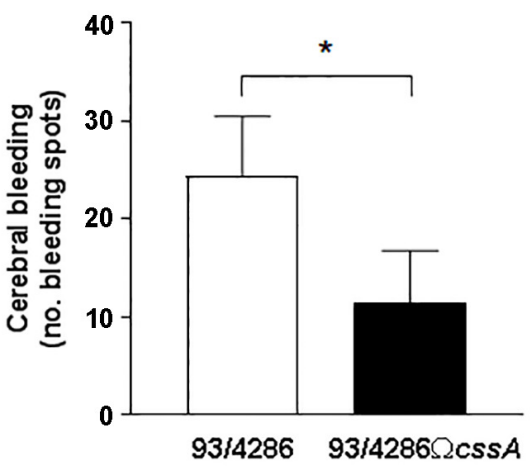




A



B



C

